Prediction of trapping rates in mixtures of partially absorbing spheres

Anuraag R. Kansal
Department of Chemical Engineering, Princeton University, Princeton, New Jersey 08544

Salvatore Torquato[a)]
Department of Chemistry, Princeton University, Princeton, New Jersey 08544

(Received 20 February 2002; accepted 27 March 2002)

The combined effects of diffusion and reaction in heterogeneous media govern the behavior of a wide variety of physical and biological phenomena, including the consumption of nutrients by cells and the study of magnetic relaxation in tissues. We have considered the so-called ''trapping problem,'' in which diffusion takes place exterior to a collection of fixed traps while reaction occurs at their surface. A simulation technique for predicting the overall trapping rate for systems of partially absorbing spherical traps based on the first-passage spheres method is presented. Using data obtained by applying this simulation technique, we then consider the problem of mixtures of partially absorbing traps. By hypothesizing a method for reducing a general mixture of traps to a mixture of perfect absorbers and perfect reflectors (i.e., reducing the dimensionality of the space of variables), we are able to accurately predict the effective surface rate constant and the trapping rate for an arbitrary mixture of partially absorbing traps. Remarkably, we find that a single, nearly universal curve allows accurate predictions to be made over a wide range of trap volume fractions and even for different trap distributions. © *2002 American Institute of Physics.*
[DOI: 10.1063/1.1479718]

I. INTRODUCTION

There are a wide variety of physical and biological systems with a simultaneously diffusing and reacting species (see, e.g., the reviews of Torquato[1] and Weiss[2]). The trapping problem is concerned with the study of these systems in the case in which the diffusing species reacts upon contact with the surface of a trapping phase. Heterogeneous catalysis, migration of defects in solids, and colloidal growth are examples of physical systems which may be modeled in this manner. The most natural biological example is the diffusion and consumption of nutrients in cells.[3,4] An area of increasing importance, however, is the study of NMR relaxation of water in biological media[5,6] (and in other, nonbiological, porous media[7–9]).

In all of these examples, the system may be divided into a pore region in which diffusion occurs and a trapping region in which the reaction takes place. Analytically, the dynamics of the trapping problem are governed by the relation

$$\frac{\partial c}{\partial t} = D\,\nabla^2 c, \tag{1}$$

in the pore phase, where c is the concentration of the diffusible species (magnetization density in NMR relaxation) and D is the diffusion constant. At the surface of the trapping region (the pore–trap interface) the diffusible species is consumed in a first-order reaction, which is modeled by the expression

$$D\frac{\partial c}{\partial n} + \kappa c = 0, \tag{2}$$

in which n is the unit outward normal to the pore region and κ is the surface rate constant. The limit of $\kappa = \infty$ corresponds to the case of instantaneous trapping (perfect absorption), while $\kappa = 0$ corresponds to complete reflection at the trap surface. The case of perfectly absorbing traps has received significant attention in the literature (e.g., Refs. 1, 2, and 10–16 and references therein). Good analytical approximations of the rate at which the diffusible species is trapped have been developed in this limit.[1,13,15,16] In addition, detailed simulations of the diffusion process have also been carried out giving ''exact'' results for a range of different trap volume fractions and spatial distributions.[14,17–19]

Trapping in systems in which the trapping reaction is finite relative to diffusion have also been investigated.[4,7,9,20–22] Because many trapping systems of physical and biological interest exist outside the diffusion-controlled regime, it is important to study the general case of arbitrary surface rate constant. A variety of techniques have been proposed ranging from analytical corrections to perfectly absorbing traps[22] to methods relying on the statistics of random walks among perfectly reflecting ''traps.''[9] In addition, results from direct simulation of random walks have also been reported.[4,7]

We report a method for the efficient simulation of diffusion and trapping based on the first-passage spheres method.[19] Using this method, we measure the trapping rate for a wide range of surface rate constants and trap volume fractions. Based on these results, we investigate the interesting problem of diffusion among mixtures of different partially absorbing traps. This choice of problem is motivated by a variety of biological phenomena. One such scenario is the situation in which several different cells populations are present in a system, each of which consumes nutrients at a

[a)]Author to whom correspondence should be addressed. Electronic mail: torquato@electron.princeton.edu

different rate. One important example in which heterogeneous cell populations arise is the growth of malignant brain tumors, which may harbor hundreds of distinct subpopulations.[23] Another system which may be modeled by a mixture of partially absorbing traps is magnetic relaxation caused by a protein molecule, in which each amino acid in the protein may relax the magnetization of bulk water at a different rate.[24]

Predicting the relaxation behavior of such a mixture poses a significant challenge because each distinct type of trap (i.e., each cell population or amino acid) has two variables associated with it (its surface rate constant and relative volume fraction). Thus, a system with all twenty amino acids would potentially be described by forty variables. By relating each type of trap to a binary mixture of perfect absorbers and reflectors, we reduce the system to one which can be described by only two variables (the total trap volume fraction and the relative proportion of perfect absorbers). Thus we reduce the dimensionality of the space of variables to only two (from forty in the case of amino acids). This method allows for the prediction of the effective surface rate constant for an arbitrary mixture of partially absorbing traps without recourse to simulations. This method is shown to be very accurate for a wide range of trap volume fractions. Notably, it also predicts the effective rate constant for mixtures in which the spatial distribution of traps is qualitatively different.

In the following section, we describe the modifications made to the first-passage spheres method to treat partially absorbing traps. In Sec. III, we present simulation results for systems with a single surface rate constant. In Sec. IV, we briefly outline results for binary systems of perfect absorbers and reflectors. The results for single surface constant systems and for the binary systems are combined to yield a method for predicting the effective surface rate constant for *arbitrary mixtures of partially absorbing traps*, and several test cases are presented. This section is followed by predictions of the effective surface rate constant for different spatial distributions of traps. Finally, we present some conclusions along with directions for further research.

II. DESCRIPTION OF ALGORITHM

The algorithm used to model three-dimensional random walks is an extension of the first-passage spheres method described initially by Torquato and Kim.[19] Briefly, the first-passage spheres method allows the motion of a particle undergoing a Brownian random walk to be simulated without explicitly simulating the fine scale details of the path. This is done by generating a sphere of radius r_i surrounding the random walker which just touches the nearest trap. The walker then moves to a location on the surface of this sphere randomly. The average time elapsed for this step, t_i, is computed using first-passage time results as

$$t_i = \frac{r_i^2}{6D}, \tag{3}$$

where D is the diffusion coefficient. This sequence is repeated until the random walker reaches a trap. Because it is impossible for the walker to actually contact the trap surface using this method, the walker is considered to have reached a trap whenever it is within some very small distance δ of the trap surface.

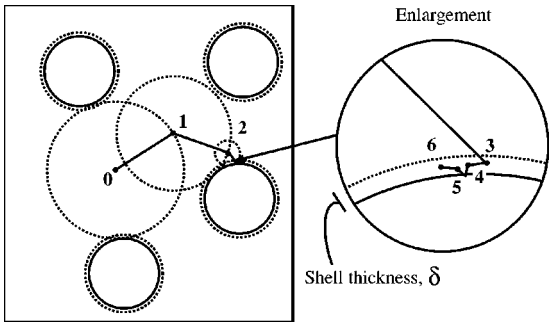

FIG. 1. Schematic of a random walker using the modified first-passage spheres method. The random walker begins at position 0. It then proceeds via first-passage spheres to position 3 (in the enlargement). At position 3 the walker is not trapped, so it proceeds with fixed steps of length δ. Note that the step from position 4 to 5 requires a reflection away from the trap surface. At positions 3 to 6 the walker is considered to have entered the trapping phase, but is not trapped until position 6. For a perfectly absorbing trap, the walker would always be trapped as soon as it enters the trapping region (at position 3 here).

In the case of perfectly absorbing traps ($\kappa=\infty$), once the walker has reached the trap, the walk ends. The mean survival time, τ for a given trap distribution is calculated as

$$\tau = \left\langle \sum_{i=1}^{\text{steps}} t_i \right\rangle, \tag{4}$$

where the the summation is taken over the steps of an individual walk and the angular brackets indicate an average over all random walks and trap realizations. For partially absorbing traps, however, the walker may not be trapped the first time it reaches a trap surface. In this situation, the first-passage spheres method needs to be modified. Specifically, a minimum-sized first-passage sphere radius is defined to be δ (the thickness of the trapping layer previously defined). The use of a minimum step size avoids computational problems associated with infinitely small step sizes. The survival time for a random walker in a system of partially absorbing traps is the sum of the time elapsed in all of the steps (including those of a fixed step length). This process is illustrated in Fig. 1. The use of finitely sized steps leads to the possibility of walkers passing into the trap area, which is not allowed in this problem. To treat this, whenever a walker reaches the trap surface, rather than continue into the trap region, it reflects away from the surface.

To determine the probability with which a walker will be trapped upon hitting the trap–pore interface, a linearization of the partially absorbing boundary condition is employed.[8] Sufficiently close to the trap surface, the trap may be treated as a plane, with diffusion taking place in one-dimension. Thus we may approximate relation (2) as

$$-D\frac{c(\epsilon)-c(0)}{\epsilon}+\kappa c(0)=0, \tag{5}$$

where $c(0)$ is the concentration at the surface and $c(\epsilon)$ is concentration a distance ϵ away from the surface. The negative sign accounts for the directionality of the normal vector. We make the approximation

$$c(0)=(1-P_\kappa)c(\epsilon), \tag{6}$$

where P_κ represents the probability that a walker contacting the trap surface is absorbed. Rearrangement yields the expression

$$\kappa=\frac{D}{\epsilon}\left(\frac{P_\kappa}{1-P_\kappa}\right), \tag{7}$$

relating the surface rate constant, κ, and the probability of a simulated walker being trapped each time it hits a trap surface, P_κ.

For the detailed random walk simulation, ϵ in relation (7) is equal to the step size. In the first-passage sphere simulations, however, this equality does not necessarily hold. This is because in the FPS simulations there is a layer in which absorption occurs, versus a surface in a direct random-walk simulation. Simulations in which the exact κ behavior is known (as discussed below) reveal that the parameter ϵ is directly proportional to δ. For the spherical trap systems considered here, $\epsilon/\delta=1.5$. The value of this ratio is independent of κ but does depend on the geometry of the traps (for example, trapping in a planar system would have a different ϵ/δ ratio).

III. IDENTICAL SPHERICAL TRAPS

We begin by investigating diffusion *interior* to isolated identical spherical cavities of radius R (i.e., the trapping phase is the region *exterior* to the cavities). In this simple case, exact solutions to (1) and (2) can be obtained.[22] In particular, the mean survival time in this system, $\tau_{\rm iso}$, is

$$\tau_{\rm iso}=\frac{R^2}{15D}+\frac{R}{3\kappa}. \tag{8}$$

This result holds for all values of κ and provides an excellent test of our algorithm. Trapping at the surface of an isolated spherical cavity of radius $R=0.1$ was simulated for a wide range of P_κ values, fixing the diffusion coefficient ($D=1$) and the boundary layer thickness ($\delta=1\times10^{-5}$). In each case, the mean survival time was calculated from the simulations and then relation (8) was used to calculate the surface rate constant, κ, corresponding to each value of P_κ. Results for eight values of P_κ varying between 0.0002 and 0.01 yielded an estimated value of 1.505 ± 0.016 for the ratio ϵ/δ. These tests were then repeated for a larger cavity ($R=0.2$), and for a thinner boundary layer ($\delta=1\times10^{-6}$), with consistent results.

With this confirmation, diffusion external to a system of impenetrable spherical traps was simulated. As discussed previously, some work in this area is available in the literature, but we have elected to perform our own simulations for several reasons. The most simple reason is that previous results do not correspond exactly to the geometry considered here. For example, in the work of Riley *et al.*,[4] diffusion can take place in the trap region, while we are interested in the case in which diffusion is confined to the pore region. Secondary reasons for using our own simulated data include ensuring that numerically precise data was available over the entire range of interest and further testing the behavior of our simulations against well-established results.

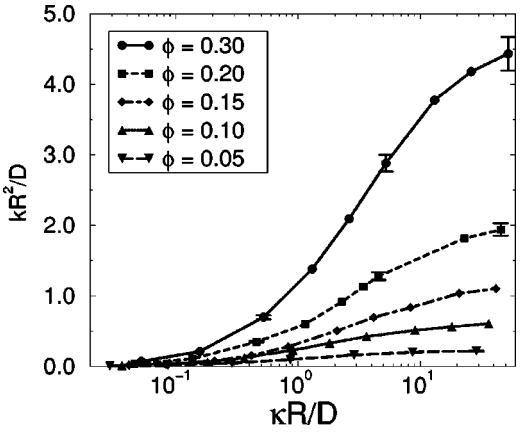

FIG. 2. Dimensionless trapping rate versus κ for several trap volume fractions. Traps are RSA distributed, nonoverlapping spheres. Averages are taken over 100 trap realizations with 1000 walkers per realization. Each realization contained 500 traps. The error bars reflect the variability between realizations. For clarity, error bars are only shown for a few combinations of κ and ϕ.

In our simulations, random realizations of spherical traps were generated using the random sequential adsorption (RSA) algorithm.[25] In the RSA method, spheres are placed one at a time. To add a sphere, the coordinates of the sphere's center are chosen randomly. The new sphere is then tested to ensure that it does not overlap with any previously placed sphere. If an overlap occurs, the new sphere is discarded and placement is attempted again. If there is no overlap, the sphere position is fixed and another sphere may then be added. This protocol has been shown to asymptotically approach a trap volume fraction of $\phi=0.38$ (in three-dimensions).[25] The traps were placed in a cube with edges of length 1. Three boundary thicknesses ($\delta=2\times10^{-5}$, 1×10^{-5}, and 5×10^{-6}) were employed and the results extrapolated to zero thickness. In practice, even the coarsest of these layers would have produced very accurate simulation data. Periodic boundary conditions were enforced. All of the traps have the same value of κ in this portion of the work.

We have tested systems of spherical traps with trap volume fractions ranging between $\phi=0.05$ and $\phi=0.30$. Values of the surface rate constant ranging from $\kappa=1$ to $\kappa=10^3$ have been investigated, along with perfectly absorbing traps ($\kappa=\infty$). The κ values are scaled by D/R to yield a dimensionless surface rate constant. Dimensionless trapping rates as a function of κ are shown in Fig. 2 for several trap volume fractions. The trapping rate, k, is defined as

$$k=1/\tau, \tag{9}$$

which is then scaled by D/R^2. Because the placement of the traps in each realization is random, the trapping rate varies between realizations. The standard deviation of this variation in the trapping rate was measured and is indicated in Fig. 2.

The standard deviation was about 4% for all combinations of κ and ϕ, and was always less than 5%. Averaging over 100 different trap realizations for each combination of the surface rate constant and trap volume fraction reduces the relative standard error to less than 1% (not indicated in the plot).

It is useful to comment briefly on the limiting behavior of the trapping rate at high and low values of κ in relation to previous research. In the high κ limit the traps become perfect absorbers. As noted previously, the system of perfect traps is a well-studied case. Comparing the results of Fig. 2 with previous studies, we find that the scaled trapping rate for high κ values approaches that of the perfectly absorbing case. As can be seen from the figure, however, traps with $\kappa = 10^3$ are not quite perfect absorbers (in which case the trapping rate curves would have saturated). To obtain a better comparison, the case of $P_\kappa = 1$ (i.e., $\kappa = \infty$) was also tested. These simulations yielded trapping rates that agreed with the results of Torquato and Kim[19] to within less than 1% deviations (data not shown).

The low κ limit corresponds to a system in which trapping is slow relative to diffusion. An optimized lower bound on mean survival time has been given by Torquato and Avellaneda as

$$\tau \geqslant \frac{\langle \delta \rangle^2}{D} + \frac{1-\phi}{2\kappa R}, \tag{10}$$

in which $\langle \delta \rangle$ is the mean pore size.[22] The data shown in Fig. 2 always respect this bound (which becomes an upper bound on the trapping rate, k). Furthermore, for $\kappa \leqslant 10$, for all values of ϕ, the bound and simulation data agree very well. This is a very stringent test of relation (7), because in the low κ limit, each walker samples the trap surface many times and any error in the calculation of P_κ will be reflected in the mean survival time.

IV. MULTIPLE κ SYSTEMS

A problem of significant biological interest is the case in which each trap has a surface rate constant assigned to it. In principle, each trap could have a unique κ value, but a more realistic scenario would be one in which a limited number of surface rate constants are present in the system. While there are many systems that can be modeled in this manner (particularly in biology), the prediction of trapping rates for mixtures of partial absorbers remains a challenging problem. In particular, mixtures of partial absorbers are characterized by a potentially large number of variables (two for each type of trap), making analytical predictions difficult.

To study this problem it is useful to begin with the simplest case—a binary system. One can envision two limiting cases for a binary system: one in which the two surface rate constants are close to one another and a second in which the two values are widely separated. In keeping with previous work on effective properties of heterogeneous media, it is reasonable to expect that the first limiting case would be somewhat easier to solve than the second. Indeed, it has been shown (albeit for a somewhat different system than considered here), that for a binary mixture of traps with two values of κ that are relatively similar, a simple arithmetic average of the trapping rate for two systems (weighted by volume fraction) each with a single surface rate constant yields a good estimate of the trapping rate of the mixed system.[4]

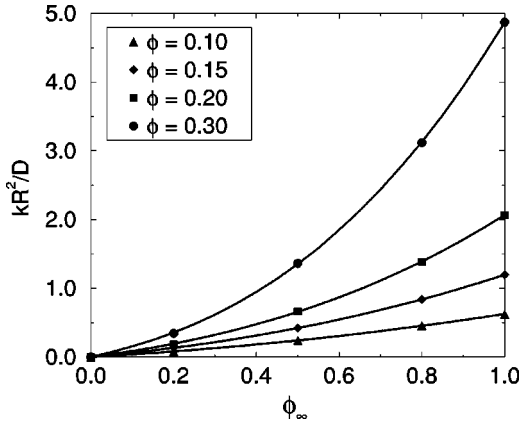

FIG. 3. The trapping rate for binary systems of perfect absorbers and perfect reflectors as a function of the fraction of absorbers. Traps are RSA distributed, monodisperse spheres. The symbols are simulation data and the lines are cubic fits to the simulation data.

As the values of κ become increasingly distinct, however, the arithmetic average begins to produce poorer results. In the limit of a mixture of perfectly absorbers and reflectors, very poor predictions should result.[4] Shown in Fig. 3 is the trapping rate (scaled as above) for systems of perfect absorbers and perfect reflectors as a function of trap volume fraction, ϕ, and the fraction of traps that are perfect absorbers, ϕ_∞. Configurations of traps are generated using the RSA algorithm and then each trap is randomly assigned to be an absorber or a reflector independently. We consider systems in which the fraction of absorbers is uniform in space. The curves in Fig. 3 are simple cubic curve fits with fixed end points. The simulation data presented is for systems with 500 traps within a periodic box. Simulations with larger numbers of traps, however, show that the scaled trapping rate, kR^2/D, is independent of the number of traps in the system at a fixed volume fraction.

One trend that can be seen from the figure is that as the overall trap volume fraction drops, the relation between the trapping rate and fraction of absorbers becomes more linear. This behavior results from the decreasing interaction between traps as the volume fraction decreases. In the limit of infinite dilution ($\phi \to 0$), each trap is independent of all others and linear behavior should be observed. While the reflectors do not trap any particles, their presence affects the trapping rate of the system as a whole. They do this by obstructing the paths between the absorbing traps. This forces diffusing particles to take longer paths (on average) before they encounter a trap, which reduces the trapping rate relative to a system with the same absorbing traps, but in which the reflectors have been removed.

While the investigation of a binary system of absorbers and reflectors demonstrates the type of behavior expected from a mixed κ system, it does not provide a direct method of understanding a system of traps with *arbitrary surface rate constants*. Even in the binary case, the behavior of mixtures of traps with intermediate surface rate constants cannot

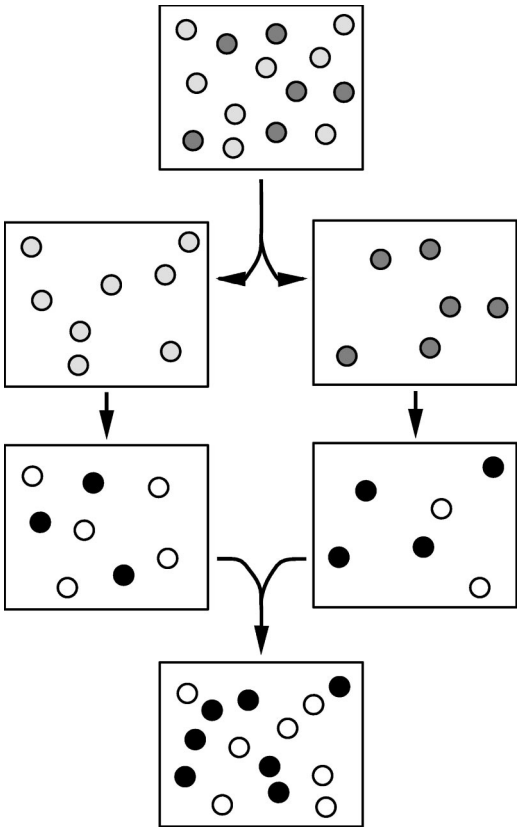

FIG. 4. Diagrammatic illustration of the mixing hypothesis underlying this work. A mixture of partially absorbing traps (at the top of the figure) may be decomposed into two systems each with a single type of partially absorbing traps. For each of these systems, a mixture of perfect absorbers and reflectors with the same trapping rate can be found. The two mixtures of absorbers and reflectors may then be combined into a third mixture of absorbers and reflectors (at the bottom of the figure). We hypothesize that the trapping rate of the original mixture of partially absorbing traps is well approximated by that of the final mixture of perfect absorbers and reflectors.

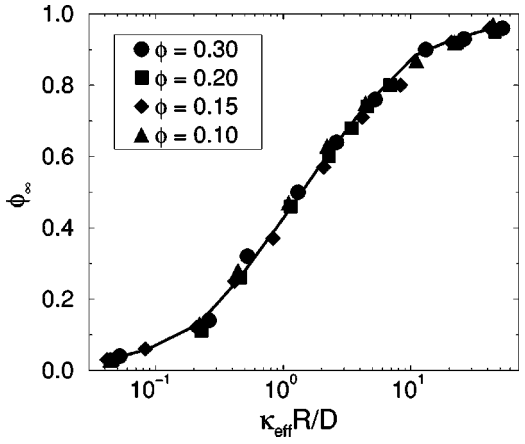

FIG. 5. The effective surface rate constant, κ_{eff}, of a binary system of perfect absorbers and reflectors, for RSA distributed traps. The fraction of absorbers in the binary system is denoted as ϕ_∞. The trap volume fraction ϕ includes both absorbers and reflectors. Note that over the range of volume fractions considered here, the dependence on volume fraction is very weak. The line is a spline fit to the data.

be predicted simply from the extreme case. However, one aspect of these simulations does indicate that they may be useful in predicting the behavior of arbitrary mixtures—the simple monotonic relationship between fraction of absorbers and trapping rate. This means that for any system of traps of arbitrary κ, there is some binary mixture of absorbers and reflectors at the same volume fraction with the same trapping rate.

This observation suggests a path for estimating the trapping rate of a mixture of traps of arbitrary values of κ based on simulations of binary systems of perfect absorbers and reflectors. Consider a binary system of traps with surface rate constants κ_a and κ_b, which we will denote as traps of type *a* and type *b*, respectively. They occupy volume fractions ϕ_a and ϕ_b, respectively, such that $\phi_a+\phi_b=\phi$. Considering only traps of type *a*, there is some binary system of perfect absorbers and reflectors at a volume fraction ϕ_a with the same trapping rate as the traps of type *a*. The same holds true for the traps of type *b*. We hypothesize that the mixture of the two binary systems of absorbers and reflectors approximates the trapping rate of the mixture of the type *a* and type *b* traps well. A schematic illustrating this hypothesis is shown in Fig. 4. While this hypothesis certainly does not hold for all cases, we will show that it is an excellent approximation in many circumstances. Note that the original mixture was characterized by four variables (κ_a, κ_b, ϕ_a, and ϕ_b), but the final binary system requires only two variables. Further, additional components in the original mixture increase the number of variables required to describe that system, the final binary system still will only require two variables to characterize. Another appealing aspect of this formulation is that it can be implemented in a straightforward manner. A single set of curves is sufficient to find the ratio of absorbers to reflectors that corresponds to a given surface rate constant in a system of partially absorbing traps. The same set of curves can then be used to find the κ_{eff} value that corresponds to the combined system of absorbers and reflectors. Finally, a set of data such as that presented in Fig. 2 can be used to predict the trapping rate based on the calculated κ_{eff}.

All of the data required to construct the plot relating a binary system of perfect absorbers and reflectors to the equivalent system with a single κ value is contained in Figs. 2 and 3. Because the curves in Fig. 3 are somewhat simpler (i.e., easier to fit well), the data points from Fig. 2 were used explicitly, while we interpolated between data points in Fig. 3. Shown in Fig. 5 is the effective surface rate constant for a binary mixture of perfect absorbers and reflectors with ϕ_∞ absorber fraction.

What stands out immediately from Fig. 5 is the very weak dependence on the trap volume fraction. In addition, the ordering with respect to the trap volume fraction is not consistent between different values of κ_{eff}, suggesting that random variations between the simulations may play a role in the scatter that is present. The significance of the scatter between the data points will be investigated in more detail below.

An intuitive understanding of the weak dependence on the trap volume fraction can be obtained from a simple example. Consider two binary systems of perfect absorbers and reflectors, with the fraction of absorbers set to $\phi_{\infty,a}$ and $\phi_{\infty,b}$. There are single κ systems with the same trapping

TABLE I. A comparison of directly measured (k_{mix}) and predicted (k_{eff}) trapping rates for mixtures of partially absorbing traps. Properties subscripted with "mix" refer to the actual mixture, while those with "eff" refer to the predicted single surface rate constant system. The traps in the actual mixture are equally divided between the set of κ_{mix} values, though in general this is not necessary. N_{trap} gives the number of traps in the system.

ϕ	N_{trap}	κ_{mix}	k_{mix}	κ_{eff}	k_{eff}	k_{eff}/k_{mix}
0.30	500	{25, 100}	753	49	773	1.03
0.30	1500	{10, 25, 50}	796	23	794	0.99
0.20	2000	{25, 100, 250}	1183	77	1198	1.01
0.15	750	{100, 250, 500}	710	220	727	1.02
0.15	1500	{10, 250, 500}	774	72	750	0.97
0.05	500	{10, 50, 250}	139	47	143	1.03
0.30	3000	{15, 20, 75, 150, 1000}	2091	59	2034	0.97

rates, with surface rate constants κ_a and κ_b, respectively. We have hypothesized that the trapping rate of the mixture of the two binary systems is well approximated by the trapping rate of a mixture of the single κ systems. If we now let the two binary systems be identical (i.e., $\phi_{\infty,a}=\phi_{\infty,b}$), the two single κ systems will also be identical. A mixture of the two binary systems, yields a binary system at the same absorber fraction, but a higher trap volume fraction. The mixture of the two single κ systems similarly yields a higher trap volume fraction with the same single κ value. By hypothesis, the two high volume fraction systems have very similar trapping rates. Because the trap volume fractions are arbitrary in this example, this suggests that the relation between the scaled trapping rate and effective surface rate constant should be *independent of the trap volume fraction*.

We have run several tests to assess how well this method can predict the effective trapping rate of a mixture of partially absorbing traps. First, the trap volume fraction and the set of surface rate constants for the mixed system were chosen. Based on Fig. 5, an effective surface rate constant was predicted. For this prediction, we used the spline curve shown in Fig. 5 for all trap volume fractions. We then simulated the mixed system and the effective system predicted and compared the resulting trapping rates. We have chosen to directly measure the trapping rate of the predicted effective system by simulation, rather than using the data presented in Fig. 2. In other words, we compare the trapping rate k_{mix} measured in a simulation of the mixture of partially absorbing spheres with the rate k_{eff} measured in a second simulation in which all spheres have a surface rate constant of κ_{eff}. This reduces the possible sources of inaccuracy in the comparisons.

The results for several tests are given in Table I. In all cases, excellent agreement was obtained between the two systems. This strongly suggests that using Fig. 2 and Fig. 5, the trapping rate for a uniform mixture of partially absorbing traps can be accurately predicted, without direct simulations. It is interesting to note that good agreement is obtained for a trap volume fraction of $\phi=0.05$, even though this volume fraction is outside the range used to create Fig. 5.

To illustrate the procedure for predicting the trapping rate for a mixture of partially absorbing spheres, consider the second test case listed in Table I ($\phi=0.30$, $N_{trap}=1500$). There are three types of traps in this mixture in equal proportion: $\kappa_a=10$, $\kappa_b=25$, and $\kappa_c=50$. Each of these subsets of traps is equivalent (in terms of trapping rate) to a binary system of perfect absorbers and reflectors, with the fraction of absorbers being $\phi_{\infty,a}$, $\phi_{\infty,b}$, $\phi_{\infty,c}$, respectively. Reading from Fig. 5, $\phi_{\infty,a}=0.25$, $\phi_{\infty,b}=0.45$, and $\phi_{\infty,c}=0.6$. Combining these three sets of binary mixtures into a single mixture yields a mixture in which the fraction of perfect absorbers is $\phi_\infty=0.43$. This is the arithmetic average of the fractions for each subset of traps, weighted by the proportion of that type of trap in the original mixture. Reading from Fig. 5 again, $\phi_\infty=0.43$ yields $\kappa_{eff}=23$.

There are several caveats to the tests made above. The first is that because no good functional form has been found to fit the data points in Fig. 5, the values have been read directly from the plot, resulting in possible measurement errors. In addition, each type of trap in the mixture must be present in sufficient number to allow it to be approximated by a binary system. For example, if only one trap has a given surface rate constant, its contribution to the trapping rate cannot be replaced by a combination of perfect absorbers and reflectors. This is essentially a finite size effect. Finally, it is important to reiterate the assumption that the different types of traps are all distributed uniformly throughout the system. If traps tend to cluster by type, markedly different behavior is expected. In this scenario, however, the majority of diffusing particles will only see traps of a single type, meaning a simple weighted average of the trapping rates for each type of trap would give a good approximation of the overall rate.

V. OTHER TRAP DISTRIBUTIONS

Noting that the effective surface rate constant for very low trap volume fractions is predicted accurately (and relying on the apparent volume fraction independence), it is natural to ask if high volume fraction systems can also be treated using this method. However, as discussed previously, trap configurations generated using the RSA protocol have a maximum volume fraction of $\phi=0.38$. In order to test higher volume fractions it is necessary to employ a different method of generating trap distributions. The simplest method is to generate configurations of traps which are allowed to overlap. The volume fraction occupied by overlapping spheres may be calculated as

$$\phi=1-\exp\left(-\rho\frac{4\pi}{3}R^3\right), \tag{11}$$

where ρ is the number density of traps in the system. While the motivation behind using the overlapping sphere system is to investigate higher trap volume fractions, several other structural features are affected. The most important is that the pore size distribution function becomes significantly altered from that of an RSA configuration. Pore size plays a key role in determining the trapping rate of a heterogeneous system in the diffusion-controlled limit.[22,26] In addition, the relationship between trap volume fraction and specific surface is different in overlapping sphere systems than in nonoverlapping systems.

The results of several test cases for overlapping traps are listed in Table II. From the table it is clear that despite the

TABLE II. A comparison of predicted trapping rates with direct simulations for partially absorbing traps using different trap distributions.

Overlapping traps						
ϕ	N_{trap}	κ_{mix}	k_{mix}	κ_{eff}	k_{eff}	k_{eff}/k_{mix}
0.26	1500	{20, 100, 500}	830	73	819	0.99
0.39	1250	{10, 25, 50}	571	23	556	0.97
0.50	1750	{10, 20, 1000}	1130	37	1093	0.97
0.63	5000	{10, 25, 50}	1700	23	1622	0.95
Equilibrated traps						
ϕ	N_{trap}	κ_{mix}	k_{mix}	κ_{eff}	k_{eff}	k_{eff}/k_{mix}
0.30	500	{10, 50, 200, 500}	808	62	828	1.02
0.40	1372	{10, 20, 1000}	1515	37	1504	0.99
0.50	500	{10, 250, 500}	2230	72	2281	1.02
0.60	1372	{10, 100, 1000}	5455	62	5172	0.95
0.72	1372	{100, 250, 500}	16 760	210	16 900	1.01
0.72	1372	{10, 25, 50}	8889	23	8163	0.92

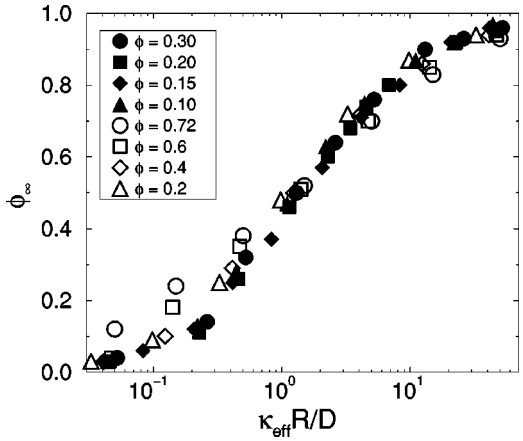

FIG. 6. A comparison of the effective surface rate constant for mixtures of perfect absorbers and reflectors between RSA distributed traps and traps arrayed on the FCC lattice. The solid symbols are data of the RSA distribution, while the open symbols correspond to the FCC lattice.

significant structural differences between overlapping traps and RSA distributed traps, reasonably accurate predictions for trapping rates can be made in the case of overlapping traps with mixed surface rate constants, using the results from the RSA systems. Note that it is necessary to explicitly measure trapping rates for single κ systems of overlapping traps as a function of the surface rate constant to quantitatively predict the trapping rate (i.e., an overlapping trap equivalent of Fig. 2 is needed), though prediction of the effective surface rate constant does not require *any* data specific to the overlapping trap system.

In order to further explore the predictive power of our method at high trap volume fractions, we have also tested nonoverlapping traps in equilibrium configurations. As the volume fraction of nonoverlapping spheres increases (at equilibrium), the system undergoes a thermodynamic phase transition. At low volume fractions, the trap distribution is liquid-like (below $\phi=0.49$), while at higher volume fractions (above $\phi=0.55$) the traps form a solid-like packing, that eventually reaches the FCC crystal. As such, by increasing the trap volume fraction, we can generate two more qualitatively different trap distributions (equilibrium liquid and solid, in addition to RSA distributed and overlapping traps). Again, we see that the effective trapping rate of mixed systems of partially absorbing traps can be predicted quite accurately.

One trend that stands out from Table II is that as the trap volume fraction increases, the predicted trapping rate generally becomes less accurate. Further, the predicted rate is systematically lower that the directly measured rate in each case in which there is a difference of 5% or more (although these cases represent a very small sample). In some regards, it is reasonable to expect that the predictions would become worse as the trap volume fraction increases. The data used in making the predictions is taken from simulations at trap volume fraction of $\phi=0.3$ and below. As predictions are made farther away from that range, they are likely to become more inaccurate. Furthermore, the structural characteristics of overlapping traps and equilibrium traps become increasingly pronounced as the trap volume fraction increases. This effect could also explain the reduced predictive power at high trap volume fractions.

In order to examine the flaws in the high volume fraction predictions in greater detail, we have studied trapping in which the traps are arrayed in an FCC lattice. By fixing the position of the traps, the variations caused by different trap configurations is eliminated. As such, the FCC lattice will also provide additional insight regarding the scatter between data points in Fig. 5 at different trap volume fractions. For this part of the study, the centers of the traps were fixed at the sites of the FCC lattice, while the size was varied to study different trap volume fractions. Trapping rates were found to be independent of the number of traps included, so all of the data presented below is obtained from simulations of 1372 traps. We repeated the methodology described above to generate a set of data analogous to Fig. 5 for FCC trap distributions. Specifically, trapping rates were calculated for a range of trap volume fractions and surface rate constants. Trapping rates were then calculated for binary systems of perfect absorbers and reflectors over the same range of trap volume fractions, for different proportions of absorbers. For each trap volume fraction, the surface rate constant was plotted against the absorber fractions that produced the same trapping rate. The resultant plot is shown in Fig. 6.

It is immediately apparent from Fig. 6 that the weak dependence on the trap volume fraction breaks down in the case of a high volume fraction and low surface rate constant. The range of volume fractions accessible using the RSA algorithm is entirely within the regime in which the volume fraction dependence is very weak. However, even for high trap volume fractions, for values of κ greater than 30 all volume fractions lie within a very narrow band. This observation suggests that trap volume fraction is responsible for some of the scatter in Fig. 5, especially at low surface rate constants. Examining the test cases in Table II, each case in which significant errors were present in the predicted trapping rate was at high volume fraction and had at least one group of traps with small κ.

VI. CONCLUSIONS

The problem of diffusing species which are trapped at the surface of a heterogeneous media has a broad range of applications. These range from heterogeneous catalysis to magnetic relaxation in NMR experiments. To date, however, the properties of systems of partially absorbing traps are only beginning to be understood in detail. Correspondingly less is known about the properties of mixed systems of partially absorbing traps.

We have adapted the first-passage sphere method for simulating diffusion among traps to treat the case of partially absorbing traps. Calibration against analytically tractable trapping problems has yielded a simple expression relating the surface rate constant, κ, in the boundary conditions of the diffusion equations and the probability that a walker is trapped in a simulation of a random walk. This modified first-passage method allows the efficient simulation of the trapping problem with partially absorbing traps. Utilizing this method, we have plotted the trapping rate for monodisperse (in both size and surface rate constant) spherical traps, versus the surface rate constant over a range of volume fractions. We chose to generate our trap configurations using the RSA protocol, which confined the trap volume fractions to be below 0.38.

In considering the overall trapping rate of binary mixtures of perfect absorbers and reflectors, a method for the prediction of the trapping rate for general mixtures was developed. This method relies on the hypothesis that the trapping rate of a mixture of several types of traps can be well approximated by a different, well-defined system of traps. This second system is comprised of subsets of traps, each of which individually displays the same trapping rate as one type of trap in the original mixture. Figure 4 shows a schematic of this hypothesis. In practice, a mixture of partially absorbing traps is decomposed into several subsets in which the surface rate constant is uniform. Each of these subsets is then approximated by a mixture of perfect absorbers and reflectors, and these mixtures are in turn combined together to yield a system whose trapping rate is approximately the same as that of the original, partially absorbing mixture. This method allows us to reduce the potentially large dimensionality of the space of variables describing a mixture of traps to only two variables. This reduction then allows for an accurate analytical estimation of the mean trapping rate.

In implementing this method, it has been found that the trap volume fraction dependence is very weak and that a single curve allows an effective surface rate constant to be predicted for an arbitrary mixture of RSA distributed, partially absorbing traps. This can in turn be used to predict the trapping rate of the original mixture. Several test cases have shown that predictions of trapping rate accurate to within 3% of the directly simulated value can be made over a broad range of trap volume fractions and surface rate constants. This includes cases in which the surface rate constants are widely separated, which is expected to be the more difficult scenario. Further trials revealed that the effective surface rate constant for other trap distributions could also be accurately predicted using the same curve. The trapping rate for systems with trap volume fractions as high as $\phi = 0.5$ can be predicted with errors of 3% or less. The traps in these systems were distributed in a variety of ways, but this did not affect the predictive power. Above these trap volume fractions, predictions became somewhat less accurate.

In summary, a nearly universal curve has been found relating the fraction of absorbers in a mixture of perfect absorbers and reflectors to the effective surface rate constant for RSA distributed traps. Using this curve, it is possible to predict the effective surface rate constant for an arbitrary mixture of partially absorbing traps. Surprisingly, the effective surface rate constant for other types of trap distributions can also be predicted accurately, despite significant structural differences. Only in the limit of a high trap fraction and small surface rate constant were predictions significantly in error.

Several questions remain open regarding the prediction of an effective surface rate constant for mixtures of traps. The most fundamental is if an analytical relation can be found for the effective surface rate constant for a mixture of perfectly absorbing and reflecting traps. This would eliminate the need to rely on tabulated relations. It also remains to be determined why the spatial distribution of the traps seems to have very little effect. It has been previously shown that a universal scaling exists for a variety of different trap geometries,[26] which may offer insight into the weak dependence of the trapping rate on spatial distribution. More broadly, one can ask what other classes of heterogeneous trapping systems could be treated using this method. For example, can an analogous analysis be found for cube shaped traps? Perfectly absorbing traps in other shapes have been studied previously,[26–28] suggesting that an extension of the methods shown here to nonspherical geometries is a tractable problem.

ACKNOWLEDGMENTS

The authors would like to thank W. Warren for valuable discussions. This work has been supported by the Engineering Research Program of the Office of Basic Energy Sciences at the Department of Energy (Grant No. DE-FG02-92ER14275).

[1] S. Torquato, J. Stat. Phys. **65**, 1173 (1991).
[2] G. H. Weiss, J. Stat. Phys. **42**, 3 (1986).
[3] P. Strove, J. Theor. Biol. **64**, 237 (1977).
[4] M. R. Riley, F. J. Muzzio, H. M. Buettner, and S. C. Reyes, Chem. Eng. Sci. **50**, 3357 (1995).
[5] K. R. Brownstein and C. E. Tarr, Phys. Rev. A **19**, 2446 (1979).
[6] R. G. Bryant, D. A. Mendelson, and C. C. Lester, Magn. Reson. Med. **21**, 117 (1991).
[7] J. R. Banavar and L. M. Schwartz, Phys. Rev. Lett. **58**, 1411 (1987).
[8] J. R. Banavar and L. M. Schwartz, in *Molecular Dynamics in Restricted Geometries*, edited by J. Klafter and J. M. Drake (Wiley, New York, 1989), pp. 273–309.
[9] M. Leibig, J. Phys. A **26**, 3349 (1993).
[10] S. Litwin, Biophys. J. **31**, 271 (1980).
[11] R. F. Kayser and J. B. Hubbard, Phys. Rev. Lett. **51**, 79 (1983).
[12] P. M. Richards, Phys. Rev. Lett. **56**, 1838 (1986).
[13] P. M. Richards, Phys. Rev. B **35**, 248 (1987).
[14] S. B. Lee, I. C. Kim, C. A. Miller, and S. Torquato, Phys. Rev. B **39**, 11833 (1989).
[15] L. Zhang and N. A. Seaton, Chem. Eng. Sci. **49**, 41 (1994).
[16] J. Rubinstein and S. Torquato, J. Chem. Phys. **88**, 6372 (1988).

[17] L. H. Zheng and Y. C. Chiew, J. Chem. Phys. **93**, 2658 (1990).
[18] L. H. Zheng and Y. C. Chiew, J. Chem. Phys. **90**, 322 (1989).
[19] S. Torquato and I. C. Kim, Appl. Phys. Lett. **55**, 1847 (1989).
[20] S.-Y. Lu, J. Chem. Phys. **110**, 12263 (1999).
[21] G. Abramson and H. Wo, Phys. Rev. E **53**, 2265 (1996).
[22] S. Torquato and M. Avellaneda, J. Chem. Phys. **95**, 6477 (1991).
[23] R. A. Berkman *et al.*, J. Neurosurg. **77**, 432 (1992).
[24] D. F. Gochberg, R. P. Kennan, M. J. Maryanski, and J. C. Gore, J. Magn. Reson. **131**, 191 (1998).
[25] D. W. Cooper, Phys. Rev. A **38**, 522 (1988).
[26] S. Torquato and C. L. Y. Yeong, J. Chem. Phys. **106**, 8814 (1997).
[27] W. Strieder, J. Chem. Phys. **112**, 2967 (2000).
[28] C. A. Miller, I. C. Kim, and S. Torquato, J. Chem. Phys. **94**, 5592 (1991).